Information Storage

DOI: 10.1002/anie.200705793

Photochemical and Electrochemical Encoding of Erasable Magnetic Patterns**

*Michael Riskin, Vitaly Gutkin, Israel Felner, and Itamar Willner**

The development of methods for the patterning of magnetic particles on surfaces attracts substantial research efforts owing to their broad technological applications in molecular electronics,[1] magnetic storage devices,[2–4] and biosensors design.[5] We report on a novel optical/electrochemical process for the generation of magnetic cobalt nanoparticle patterns on a functional monolayer. The magnetic nanoparticle patterns are erasable giving an encoded nanostructure that can regenerate the magnetic patterns by an electrochemical transformation. The electroswitchable formation and dissociation of the magnetic patterns enable the dynamic reversible transition of the magnetic structures from a microscale pattern to a nanoscale pattern. The fabrication of signal-controlled "smart surfaces" attracts considerable interest because of the potential uses of these systems as self-cleaning surfaces, microfluidic transport of liquids, switchable catalysts, and information storage and processing systems.

The electrical control of the hydrophobic and hydrophilic properties of surfaces has been achieved by the dynamic bending of charged monolayers[6,7] or by the electrochemical shuttling of molecular components on molecular wires in a monolayer structure.[8] Also, switching the redox states of a monolayer associated with a surface has enabled the microfluidic delivery of liquids by capillary forces.[9] Similarly, the light-induced isomerization of monolayers between redox-active and redox-inactive structures has been suggested as a means for optical information storage, with the readout performed by electrochemical methods.[10,11] Also, electrochemical shuttling of molecular components on functional monolayer wires provides the basis for ultra-dense information storage systems.[12] Magnetic nanoparticles (NPs) provide a promising material for information storage, and the formation of nanostructures of particles on surfaces is a prerequisite for such devices.[13–15] Different techniques have been developed to pattern magnetic NPs onto surfaces, including electron-beam lithography,[16] microcontact printing,[17] scanning tunneling microscope lithography,[18] dip-pen nanolithography,[19] and electrochemical etching followed by electrodeposition.[20] Herein we describe a method to address magnetic Co NPs to a photoisomerizable monolayer associated with an electrode. The resulting magnetic pattern can be erased and regenerated by electrochemical means. We also demonstrate that under an applied magnetic field, the repeated electrochemical breakdown and formation of the magnetic NPs leads to a dynamic transition of the magnetic microstructures into nanostructures.

Previously, the association of metal ions to a thiolated monolayer linked to an electrode has been used to enable the cyclic electrochemical formation of metallic nanoclusters on the surface and their electrochemical breakdown to ions that were confined to the monolayer-functionalized electrode.[21,22] Also, a photoisomerizable monolayer has been used for optically addressing of Ag^+ ions to the nitromerocyanine photoisomer state of the monolayer.[23] The electrochemical reduction of the Ag^+ ions associated with the monolayer generated Ag^0 nanoclusters that could be re-oxidized to the Ag^+ ions, and by the photoisomerization of the nitromerocyanine monolayer to the nitrospiropyran state, the Ag^+ ions could be washed off from the electrode surface.

Mercaptobutyl nitromerocyanine (**1**) was assembled as a monolayer on a Au electrode. The resulting monolayer could be reversibly photoisomerized between the nitromerocyanine (**1a**) and nitrospiropyran (**1b**) states (Scheme 1). After binding of Co^{2+} ions to the **1a**–monolayer state, the Co^{2+} ions were electrochemically reduced to Co^0 NPs ($E = -0.95$ V vs. Ag/AgCl, Figure 1 A). Upon applying a potential of -0.2 V (vs. Ag/AgCl), the Co^0 nanoclusters were re-oxidized to Co^{2+} ions. By the coulometric analysis of the oxidation wave of Co^0, the surface coverage of Co^{2+} ions was estimated to be 1.4×10^{-10} mol cm^{-2}. It should be noted that at the peak-reduction potential of the Co^{2+} ions (-0.95 V vs. Ag/AgCl) the thiolated monolayer might be partially reductively desorbed. However, in the absence of Co^{2+} ions we did not observe any desorption wave at this potential. In all the other experiments we applied a limiting negative potential of -0.88 V vs. Ag/AgCl for a time interval of 2 min. We find that after this time interval the oxidation peak of the Co^0 nanoclusters is almost overlapping the peak shown in the cyclic voltammogram, Figure 1 A. These results indicate that the applied potential step reduces all the Co^{2+} ions associated to the monolayer, while ensuring that the rest of the

[*] M. Riskin, Prof. I. Willner
The Institute of Chemistry
The Hebrew University of Jerusalem
91904 Jerusalem (Israel)
Fax: (+972) 2-652-7715
E-mail: willnea@vms.huji.ac.il
V. Gutkin
The Unit for Nanocharacterization
The Center for Nanoscience and Nanotechnology
The Hebrew University of Jerusalem, Faculty of Science
E.Safra Campus, Givat Ram, 91904 Jerusalem (Israel)
Prof. I. Felner
Racah Institute of Physics
The Hebrew University, 91904 Jerusalem (Israel)

[**] Support from the Israel Science Foundation as a NanoScience European NanoSci-Era project (NANOLICHT) and the CAMBR Company research fellowship (M.R.) are acknowledged.

Supporting information for this article is available on the WWW under http://www.angewandte.org or from the author.

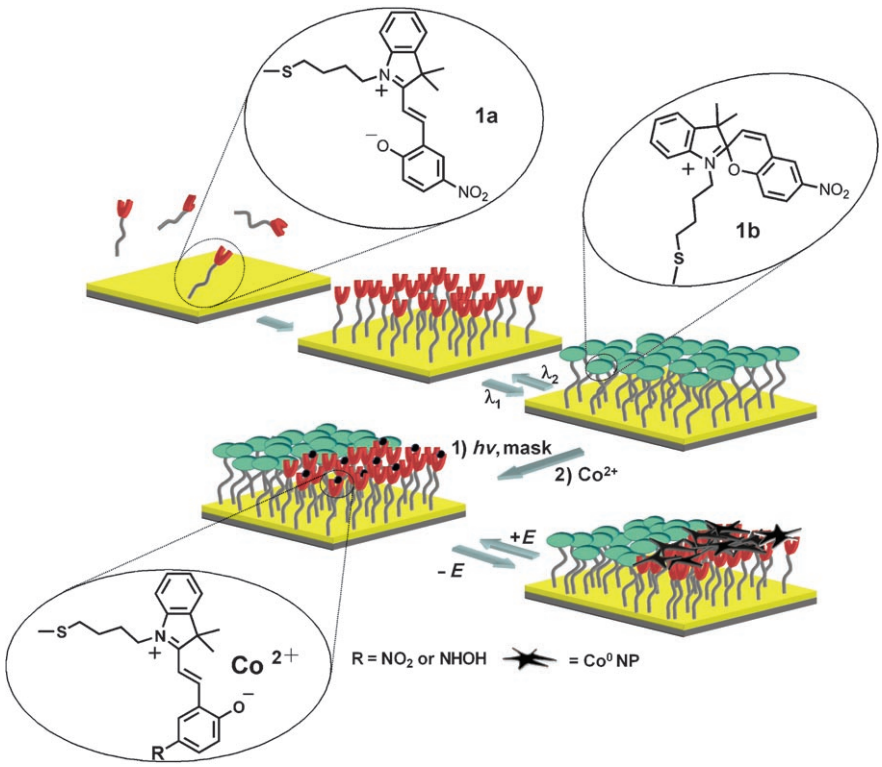

Scheme 1. Photochemical encoding and readout of magnetic patterns on a photoisomerizable monolayer associated with a gold electrode, and the subsequent erasure of the patterns while retaining the encoded information (see text for details).

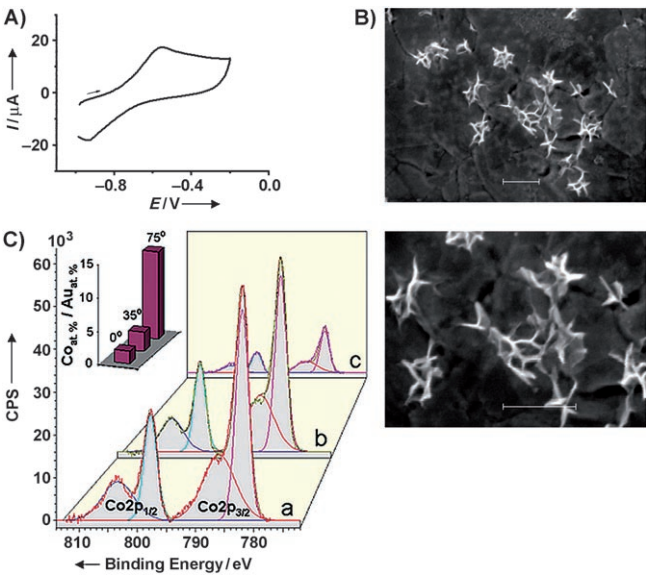

Figure 1. A) Cyclic voltammogram of the Co^{2+} ions linked to the merocyanine-monolayer-functionalized electrode; scan rate 20 $mV s^{-1}$, electrolyte composition: 0.05 M K_2SO_4, pH 7.4. B) SEM images of the electrogenerated Co^0 nanoclusters linked to the merocyanine-monolayer-functionalized Au electrode; scale bars 200 nm. C) Angle-dependent XPS spectra of the Co^0–NP-functionalized surface. The letters a, b, and c correspond to the Co doublet spectra at take-off angles of 0, 35, and 75°, respectively. Inset: Atomic concentrations ratio of the Co/Au support at different take-off angles.

monolayer is not disrupted. X-ray photoelectron spectra confirmed the transformation of the Co^{2+} to Co^0. Figure 1B depicts the SEM images of the resulting Co^0 star-like nanoclusters. They have an average diameter of 40–50 nm, and the thickness of the Co "arms" is 3.0–4.0 nm. From the SEM images, we estimate that approximately 10 to 15% of the Au surface is covered by the Co^0 nanoclusters. This surface density agrees well with angle-dependent X-ray photoelectron spectra (XPS) measurements on the Co^0-functionalized surface (Figure 1C). The measurements confirmed the transformation of the Co^{2+} to Co^0. The angle-dependent XPS of the patterned surface reveals that the doublet signal of cobalt ($2p_{1/2}$, $2p_{3/2}$), and the relative intensities of the cobalt doublet bands (Figure 1C, inset) strongly increase as the beam angle becomes closer to the grazing angle. Analysis of the XPS intensities indicates an average thickness of the Co^0 nanoclusters layer of approximately 6 nm that translates to an approximately 12% coverage of the surface by the 50-nm-sized nanoclusters.

Figure 2A shows the $M(T)$ curve measured at 1 kOe of the resulting Co^0-nanocluster-functionalized surface. While the magnetic moment M is almost constant in the range of 20–110 K, a sharp transition is observed at 130 K, a behavior characteristic to a ferromagnetic substance. The increase below 20 K is due to paramagnetic Co^{2+} ions which obey the Curie–Weiss (CW) law: $\chi(T) = \chi^0 + C/(T-\theta)$, where χ^0 is the temperature-independent part of χ, C is the Curie constant, and θ is the CW temperature. The least-square fit of the $\chi(T)$ yields $C = 2.37 \times 10^{-7}$ emu kOe^{-1}, and $\theta = 4.4$ K.

The electron-transfer rates for the reduction of the Co^{2+} ions to the Co^0 nanoclusters, and the reversed oxidation of the Co^0 nanoclusters to Co^{2+} ions were characterized by chronoamperometry and complementary surface plasmon resonance (SPR) measurements. Figure 2B, curve a shows the cathodic current transient observed upon the reduction of the Co^{2+} ions to Co^0. The derived electron-transfer-rate constant is 1200 s^{-1}. Figure 2B, curve b, depicts the anodic current transient upon the oxidation of the Co^0 nanoclusters to the Co^{2+} ions. The derived electron-transfer-rate constant is 740 s^{-1}. The coupling of the magnetic moment of the particles with the plasmon wave of the Au surface[24] as well as the changes of the dielectric properties of the surface as a result of the transition of Co^{2+} ions to Co^0 and back, affect the SPR spectra of the Au surface. Figure 2C, curve a, shows that the time-dependent SPR changes upon the reduction of the Co^{2+} are substantially slower than the reduction rate observed by chronoamperometry. This apparent discrepancy is attributed

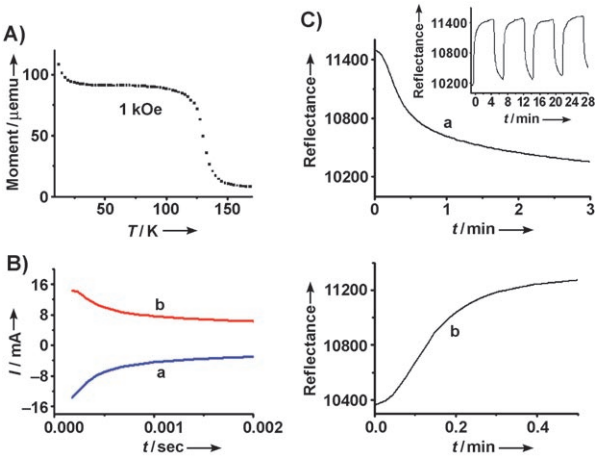

Figure 2. A) Temperature-dependent magnetization of the Co^0-nanocluster-functionalized Au surface. B) Chronoamperometric transients corresponding to: a) The reduction of the Co^{2+} to Co^0 upon the application of a potential step from −0.2 V to −0.88 V. b) The oxidation of the Co^0 nanoclusters to Co^{2+} upon the application of a potential step from −0.88 V to −0.2 V. C) a) The sensogram corresponding to the reflectance changes upon the reduction of the Co^{2+} to Co^0 upon the application of a potential step from −0.2 V to −0.88 V. Inset: Cyclic reflectance changes upon switching the potential between −0.88 V and −0.2 V. b) The sensogram corresponding to the reflectance changes upon the oxidation of the Co^0 nanoclusters to Co^{2+}, applied potential step from −0.88 V to −0.2 V (all potentials vs. Ag/AgCl).

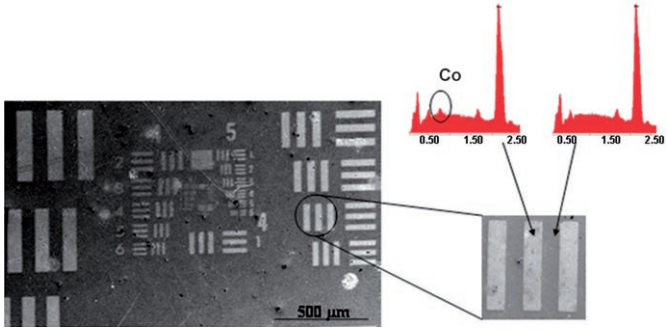

Figure 3. Pattern of Co^0 nanoclusters generated upon electrochemical reduction of Co^{2+} ions bound to a photogenerated nitromerocyanine pattern on a Au surface (left). The right image depicts the EDS spectra (red) of the nitrospiropyran domain (dark areas) and Co^0 NPs patterned area (light areas), respectively.

to the fact that chronoamperometry monitors the reduction of Co^{2+} ions to Co^0 atoms, whereas the changes in the SPR spectra monitor the clustering rates of the Co^0 atoms to the NPs. Figure 2C, curve b, implies that, upon the oxidation of the Co^0 NPs, the re-distribution of the Co^{2+} ions on the merocyanine monolayer is fast. The changes in the SPR spectra upon the reduction of the Co^{2+} ions to Co^0 nanoclusters, and the re-oxidation of the clusters are fully reversible (Figure 2C, inset). Control experiments show that no changes in the SPR spectra are observed upon application of the potential steps to the **1a**-modified electrode in the absence of Co^{2+} ions. These results demonstrate that the ions and nanoclusters are confined to the monolayer upon undergoing the respective redox processes. Similar kinetic results were observed for the electrochemically induced nanoclustering of Ag^0 or Hg^0 nanoparticles on monolayers and for their electrochemical breakdown on the monolayer-functionalized electrodes.[22] The electrochemical reduction of the Co^{2+} ions to Co^0 NPs and the re-oxidation of the nanoclusters to the Co^{2+} ions is fully reversible, showing that the Co^{2+} ions as well as the Co^0 NPs are confined to the monolayer, and they do not dissociate into the electrolyte solution.

Irradiation of the monolayer in the nitrospiropyran state (**1b**), through a mask, $320 < \lambda < 360$ nm, resulted in the selective formation of the nitromerocyanine pattern (**1a**).[25] Treatment of the surface with the Co^{2+} solution resulted in the association of the Co^{2+} ions only to the nitromerocyanine sites (**1a**; Scheme 1). The subsequent electrochemical reduction of the Co^{2+} ions yielded a magnetic pattern composed of the Co^0 NPs (Figure 3). The magnetic patterns could be reversibly erased and then regenerated by the electrochemical oxidation of the Co^0 NPs to Co^{2+} and the subsequent reduction of the Co^{2+} ions to the Co^0 NPs, respectively. These results indicate that the Co^{2+} ions are confined to the nitromerocyanine domains. Indeed, EDS measurements confirmed that the Co^{2+} ions are localized at the nitromerocyanine regions and lack any binding to the nitrospiropyran domains. (The atomic concentration of Co 2p signals associated with the (**1a**) and (**1b**) surface domains corresponded to 7.55% and 0.0%, respectively).

It should be noted that in the absence of cobalt species the photogenerated nitromerocyanine (**1a**) patterns can be erased by irradiation of the surface with visible light, resulting in photochemical isomerization to the nitrospiropyran (**1b**) state. However, the binding of the Co^{2+} ions to the nitromerocyanine pattern, and the subsequent reduction of the ions to the Co^0 NPs, yields a nitromerocyanine pattern that cannot be erased. Thus, although the magnetic pattern is erasable, the nitromerocyanine monolayer has lost its photoisomerization properties, that is, the **1a**⇄**1b** photoisomerization is no longer possible. This change in the photoisomerization properties occurs because at the potential at which the Co^{2+} ions are reduced, $E = -0.95$ V vs. Ag/AgCl, the nitro functionalities of the **1a** units in the monolayer are reduced to hydroxylamine functionalities, yielding a non-photoisomerizable spiropyran product.[26]

The reversible electrochemical formation and breakdown of the magnetic particles and the confinement of the Co^{2+} ions to the photopatterned domains enable further structural manipulation of the magnetic pattern by the application of an external magnetic field (Figure 4). When an external magnet is placed in a pre-defined position in respect to the original magnetic NP pattern, the cyclic electrochemical breakdown of the Co^0 NPs and the re-reduction of the Co^{2+} ions to the Co^0 NPs result in the magnetic NPs being collected by the external magnet. Figure 4A depicts the collection and the shrinking of the 24.8×124 μm pattern of the Co^0 NPs upon placing the external magnet at the bottom of the pattern in a perpendicular orientation, while applying 25 reduction/oxidation cycles to the Co^{2+}/Co^0 species. The original pattern shrinks to dimensions corresponding to 24.8×35 μm. EDS

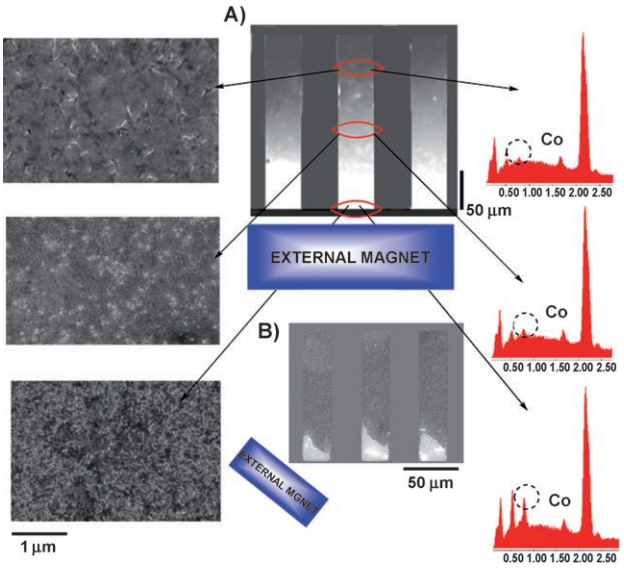

Figure 4. External magnetic field effects on the electrogenerated magnetic patterns associated with the photopatterned nitromerocyanine regions. A) Collection of the magnetic Co^0 nanoparticles associated with the 24.8×124 μm nitromerocyanine domain by the application of 25 reduction/oxidation cycles of Co^{2+} to Co^0 and back, scan rate 20 $mV s^{-1}$, while positioning the magnet below the pattern. Right side: EDS spectra of Co nanoclusters, left side: SEM images of the different domains on the photolithographed pattern. B) Collection of the magnetic Co^0 nanoparticles associated with the nitromerocyanine monolayer upon positioning the external magnetic field direction at 45° with respect to the photolithographed pattern. The magnetic particles were collected by applying 25 reduction/oxidation steps, 20 $mV s^{-1}$. The strength of the external magnetic field is 1.6 T.

and SEM measurements confirm the collection of the magnetic particles by the external magnet. Similarly, a 2.2 × 11 μm Co NPs pattern was transformed to a 0.5 μm × 11 μm nanostructure of the particles. Figure 4B shows the conversion of a 24.8 × 124 μm Co NPs pattern into a triangle shaped miniaturized magnetic domain by the angular positioning of the external magnet in respect to the pattern and the electrochemical cycling of the reduction/oxidation of the Co^{2+}/Co^0 species (25 cycles).

In conclusion, we have shown the photo-addressed formation of erasable magnetic patterns. We highlight the formation of a "smart surface" where the optical information is encoded by generating a nitromerocyanine pattern which acts as a template for the subsequent binding of Co^{2+} ions to these surface-confined structures. The encoded information is then readout by the electrochemical conversion of the layer into magnetic NPs-functionalized patterns. This magnetic information could be erased by electrochemical breakdown of the particles, but the encoded information was still retained in the system, and the Co^0 NP patterns could be regenerated on demand. Thus, the patterned Co^{2+} ions associated with the surface might act as a "secret ink". The encoded information might be retrieved at any time by the electrochemically induced generation of the magnetic pattern, and this may be subsequently erased by an electrical signal, while retaining the encoded information. Besides the functions of the assembly as a write–read–erase system, the ability to manipulate the magnetic pattern by means of an external magnet demonstrated the cyclic dynamic control of the shapes and dimensions of the magnetic structures on surfaces.

Experimental Section

The different instruments and experimental conditions used to characterize the electrochemical, magnetic, and microscopy features of the surfaces are detailed in the supporting information.

Modification of Au surfaces: Au-Coated (50 nm gold layer) glass plates (22 × 22 mm^2; Evaporated Coatings, PA, USA) were flame-annealed for 5 min in a *n*-butane flame and cooled for 10 min under a gentle stream of Ar. The resulting plates were placed in an ethanol solution of **1** (1 mM) for 2 h. The resulting monolayer-functionalized surface was then washed with ethanol and water and dried. Subsequently, the surface was irradiated with visible light ($\lambda >$ 475 nm) to produce the **1b**-monolayer state. The electrode was immersed in a 0.05 M Na_2SO_4 solution, pH 8.1, and irradiated through a mask with long-wave UV light $320 < \lambda < 360$ nm, resulting in the pattern of **1a** in the light-exposed areas. The resulting surface was then immersed in an aqueous solution of 0.05 M Na_2SO_4, pH 8.1, that included 20 mM $Co(NO_3)_2$ for 6 h. The surface was washed with water, dried with nitrogen and cycled 5-10 times in an electrolyte solution of 0.05 M K_2SO_4, pH 7.4, scan rate 20 $mV s^{-1}$, in order to exclude the presence of non-specifically adsorbed Co^{2+} ions.

Received: December 18, 2007
Published online: April 24, 2008

Keywords: electrochemistry · magnetic nanoparticles · nanostructures · patterning · photolithography

[1] G. A. Prinz, *Science* **1998**, *282*, 1660.
[2] H. Ohno, D. Chiba, F. Matsukura, T. Omiya, E. Abe, T. Dieti, Y. Ohno, K. Ohtani, *Nature* **2000**, *408*, 944.
[3] S. P. Li, D. Peyrade, M. Natali, A. Lebib, Y. Chea, U. Ebels, L. B. Buda, K. Ounadjela, *Phys. Rev. Lett.* **2001**, *86*, 1102.
[4] R. L. White, *J. Magn. Magn. Mater.* **2002**, *242*, 21.
[5] R. L. Edelstein, C. R. Tamanaha, P. E. Sheehan, M. M. Miller, D. R. Baselt, L. J. Whitman, R. J. Colton, *Biosens. Bioelectron.* **2000**, *14*, 805.
[6] J. Lahann, S. Mitragotri, T-N. Tran, H. Kaido, J. Sundaram, I. S. Choi, S. Hoffer, G. A. Somorjai, R. Langer, *Science* **2003**, *299*, 371.
[7] X. Wang, A. B. Kharitonov, E. Katz, I. Willner, *Chem. Commun.* **2003**, 1542.
[8] E. Katz, O. Lioubashevsky, I. Willner, *J. Am. Chem. Soc.* **2004**, *126*, 15520.
[9] N. L. Abbott, G. M. Whitesides, *Langmuir* **1994**, *10*, 1493.
[10] Z. F. Liu, K. Hashimoto, A. Fujishima, *Nature* **1990**, *347*, 658.
[11] A. Doron, M. Portnoy, M. Lion-Dagan, E. Katz, I. Willner, *J. Am. Chem. Soc.* **1996**, *118*, 8937.
[12] C. P. Collier, G. Mattersteig, E. W. Wong, Y. Luo, K. Beverly, J. Sampaio, F. M. Raymo, J. F. Stoddart, J. R. Heath, *Science* **2000**, *289*, 1172.
[13] H. Zeng, J. Li, Z. L. Wang, J. P. Liu, S. Sun, *Nature* **2002**, *420*, 395.
[14] E. V. Shevchenko, D. V. Talapin, A. L. Rogach, A. Kornowski, H. Haase, H. Weller, *J. Am. Chem. Soc.* **2002**, *124*, 11480.
[15] D. J. Sellmyer, M. Yu, R. D. Kirby, *Nanostruct. Mater.* **1999**, *12*, 1021.
[16] M. S. Wei, S. Y. Chou, *J. Appl. Phys.* **1994**, *76*, 6679.
[17] S. Palacin, P. C. Hidber, J.-P. Bourgoin, C. Mivamond, C. Fermon, G. M. Whitesides, *Chem. Mater.* **1996**, *8*, 1316.
[18] A. D. Kent, T. M. Shaw, S. von Molnar, D. D. Awschalom, *Science* **1993**, *262*, 1249.

[19] X. Liu, L. Fu, S. Hong, V. P. Dravid, C. A. Mirkin, *Adv. Mater.* **2002**, *14*, 231.
[20] S. A. Gusev, N. A. Korotkova, D. B. Rozenstein, A. A. Fraerman, *J. Appl. Phys.* **1994**, *76*, 6671.
[21] a) M. Manolova, V. Ivanova, D. M. Kolb, H.-G. Boyen, P. Ziemann, M. Buettner, A. Romanyuk, P. Oelhafen, *Surf. Sci.* **2005**, *590*, 146; b) V. Ivanova, T. Baunach, D. M. Kolb, *Electrochim. Acta* **2005**, *50*, 4283; c) T. Baunach, V. Ivanova, D. M. Kolb, H.-G. Boyen, P. Ziemann, M. Buettner, P. Oelhafen, *Adv. Mater.* **2004**, *16*, 2024.
[22] a) M. Riskin, B. Basnar, V. I. Chegel, E. Katz, I. Willner, F. Shi, X. Zhang, *J. Am. Chem. Soc.* **2006**, *128*, 1253; b) M. Riskin, B. Basnar, E. Katz, I. Willner, *Chem. Eur. J.* **2006**, *12*, 8549.
[23] M. Riskin, E. Katz, V. Gutkin, I. Willner, *Langmuir* **2006**, *22*, 10483.
[24] N. Bonod, R. Reinisch, E. Popov, M. Neviere, *J. Opt. Soc. Am. B* **2004**, *21*, 791.
[25] A. Doron, E. Katz, G. Tao, I. Willner, *Langmuir* **1997**, *13*, 1783.
[26] E. Katz, M. Lion-Dagan, I. Willner, *J. Electroanal. Chem.* **1995**, *382*, 25.

